Published online 9 October 2017 *Nucleic Acids Research, 2017, Vol. 45, No. 21* ***12481–12495***
doi: 10.1093/nar/gkx912

The RNA binding protein EWS is broadly involved in the regulation of pri-miRNA processing in mammalian cells

Huiwu Ouyang[1], Kai Zhang[1], Kristi Fox-Walsh[2], Yang Yang[1], Chen Zhang[1], Jie Huang[1], Hairi Li[2], Yu Zhou[1,3,*] and Xiang-Dong Fu[1,2,*]

[1]State Key Laboratory of Virology and Hubei Key Laboratory of Cell Homeostasis, College of Life Sciences, Wuhan University, Wuhan 430072, China, [2]Department of Cellular and Molecular Medicine, Institute of Genomic Medicine, University of California, San Diego, La Jolla, CA 92093-0651, USA and [3]Institue of Advanced Studies, Wuhan University, Wuhan 430072, China

Received December 12, 2016; Revised September 07, 2017; Editorial Decision September 26, 2017; Accepted September 27, 2017

ABSTRACT

The Ewing Sarcoma protein (EWS) is a multifaceted RNA binding protein (RBP) with established roles in transcription, pre-mRNA processing and DNA damage response. By generating high quality EWS–RNA interactome, we uncovered its specific and prevalent interaction with a large subset of primary microRNAs (pri-miRNAs) in mammalian cells. Knockdown of EWS reduced, whereas overexpression enhanced, the expression of its target miRNAs. Biochemical analysis revealed that multiple elements in target pri-miRNAs, including the sequences flanking the stem–loop region, contributed to high affinity EWS binding and sequence swap experiments between target and non-target demonstrated that the flanking sequences provided the specificity for enhanced pri-miRNA processing by the Microprocessor Drosha/DGCR8. Interestingly, while repressing Drosha expression, as reported earlier, we found that EWS was able to enhance the recruitment of Drosha to chromatin. Together, these findings suggest that EWS may positively and negatively regulate miRNA biogenesis via distinct mechanisms, thus providing a new foundation to understand the function of EWS in development and disease.

INTRODUCTION

EWS belongs to the TET family of RNA binding proteins (RBPs), consisting of FUS/TLS, EWS, and TAF15 (1,2). These RBPs have been implicated in multiple layers of regulated gene expression via their roles in modulating transcription (3–6), coupling between transcription and RNA processing (7) and mediating splice site selection during pre-mRNA splicing (8–11). Consequently, knockout of these RBPs causes severe developmental abnormality in mice (12,13). Importantly, various chromosome translocation events that involve *EWS* and mutations in both *EWS* and *FUS/TLS* have been linked to specific human diseases (14,15).

Given the ability of individual TET family members to bind RNAs, multiple groups have performed crosslinking immunoprecipitation coupled with deep sequencing (CLIP-seq) to characterize their RNA binding profiles on both cellular and animal models (16,17). The initial analysis by PAR-CLIP on HEK293 cells showed related, but distinct RNA binding profiles of FUS/TLS, EWS and TAF15 (18). This study also revealed a general association of these RBPs with 3′ splice sites in pre-mRNAs and a preference for both G-rich and AU-rich sequences. However, the association of these RBPs with 3′ splice sites was not seen by a separate CLIP study of EWS on HeLa cells, which instead showed enriched RNA binding near EWS-regulated 5′ splice sites (10). Two independent genome-wide analyses of FUS/TLS in mouse and human brain also found its prevalent coating on long pre-mRNA transcripts; however, most binding events detected in these studies did not seem to occur near induced alternative splicing events in FUS/TLS deficient cells (8,11). While it has been unclear about the sources of such discrepancies, the seemly degenerative sequence preference for the TET family members might be explained by the observation that FUS/TLS appears to bind certain secondary structures in RNAs, rather than specific motifs in exposed single-stranded RNA regions (18). More importantly, the biological meaning of most detected RNA binding events has been poorly understood.

We were initially motivated to investigate various inconsistencies among published genome-wide RNA inter-

*To whom correspondence should be addressed. Tel: +1 858 534 4937; Email: xdfu@ucsd.edu
Correspondence may also be addressed to Yu Zhou. Tel: +86 27 68756749; Email: yu.zhou@whu.edu.cn

actomes by the TET family members. Instead of relying on mining the existing datasets, we generated our own high quality EWS CLIP-seq libraries on HeLa cells and noted prevalent interaction of EWS with a large number of expressed pri-miRNAs, reminiscent of FUS/TLS binding to hairpin-containing RNAs as reported earlier (18). We therefore decided to focus on this new lead in the current study because it has been reported that a large number of miRNAs were induced while others suppressed in EWS knockout mouse embryonic fibroblasts (MEFs) (19). Interestingly, EWS deficiency has also been linked to elevated Drosha expression at both the mRNA and protein levels, and because Drosha is the catalytic subunit of the Microprocesssor, which is recruited to chromatin to facilitate co-transcriptional pri-miRNA processing in the nucleus (20,21), increased Drosha may therefore account for the induction of a specific set of miRNAs (19). However, how EWS deficiency would also cause the repression of other miRNAs has remained unknown.

We now provide evidence for a direct role of EWS in enhancing pri-miRNA processing by the Microprocessor, thus joining EWS to the growing list of RBPs involved in modulating miRNA biogenesis in mammals (22–24). Unlike other RBPs involved in modulating miRNA biogenesis described earlier, EWS appears to bind and modulate processing of a large number of pri-miRNAs. Coupled with EWS-mediated Drosha repression, this RBP appears to be capable of both stimulating and inhibiting miRNA biogenesis, but via distinct mechanisms, which we have dissected in this study. The newly elucidated function of EWS adds a new dimension in understanding the mechanisms underlying EWS mutation-induced cancers (5,25,26) and neurodegenerative diseases (27).

MATERIALS AND METHODS

Cell culture, transfection, antibodies, RT-qPCR of miRNAs

HeLa cells were grown in Dulbecco's modified Eagle's medium (DMEM) supplemented with 10% newborn bovine serum (Gibco) at 37°C in 5% CO_2. RNAimax and Lipo2000 (Life Technology) were used for siRNA and plasmid transfection, respectively, according to manufacturer's instructions. The siRNA against Drosha (5′-AACGAGUAGGCUUCGUGACUU-3′) was prepared based on published sequences (28), and two independent siRNAs against EWS (5′-AUGAUCUGGCAGACUUCUUUA-3′; 5′-AGCGAGGUGGCUUCAAUAAGC-3′) were according to the siRNA database (29). Antibodies for specific experiments described in the Results section were purchased from various vendors: anti-Drosha (Abcam, ab12286), anti-DGCR8 (Proteintech, 10996-1-AP), anti-EWS (Proteintech, 55191-1-AP), anti-Myc (Proteintech, 60003-2-Ig), anti-eGFP (Proteintech, 66002-1-Ig), anti-actin (ABclonal, AC004), anti-FLAG tag (Proteintech, 66008-2-Ig).

The miScript PCR Starter Kit (Qiagen, 218193) was used to quantify miRNAs. After Trizol extraction of total RNA, mature miRNAs were polyadenylated by poly(A) polymerase and reverse transcribed into cDNAs by using an oligo-dT primer provided in this kit. The oligo-dT primer contains a 3′ degenerate anchor and a universal tag sequence at the 5′ end, allowing quantitative analysis of mature miRNA by real-time PCR using the universal primer and a miRNA-specific primer. Quantitative PCR was carried out with 1:100 dilution cDNA, 2× SYBR Green PCR Mix, 10× miScript universal primers included in the kit, in combination with 10× miRNA specific primers (listed in Supplementary Table S1). The U6 snRNA primer from Qiagen was used for normalization and ΔCt was calculated to derive relative expression.

Plasmid construction, luciferase assay, protein purification

Myc-tagged EWS cDNA at the N-terminus was generated by PCR using specific primers (listed in Supplementary Table S2) and inserted into pcDNA3.0 between EcoR I and Xho I sites for EWS overexpression in transfected HeLa cells.

For MS2-based capture experiments, the MS2 stem–loop sequence was excised from the plasmid 5U3M described previously (30) by restriction digestion with Hind III and Xho I, ligated to PCR-amplified pri-miRNA containing the Xho I and Not I sites, and then inserted the product into pcDNA3.0 at Hind III and Not I sites. The plasmid for expressing the EGFP-MS2 fusion protein was as described previously (30). The primers used in MS2-Pri-miRNA plasmid construction are listed in Supplementary Table S2.

To construct the Renilla luciferase reporters for measuring pri-miRNA processing in transfected cells, individual pri-miRNA sequences were first PCR amplified by using specific primers (listed in Supplementary Table S2) and cloned into psiCHECK™-2 Renilla 3′UTR between the Xho I and Not I sites.

Pri-miRNAs used for gel shift and *in vitro* processing assays were all transcribed from pcDNA3.0 clones containing individual pri-miRNAs generated by PCR using specific primers (listed in Supplementary Table S2). To construct various chimeric pri-miRNA plasmids, individual fragments were PCR amplified from the pcDNA3.0-pri-miR-222 or pcDNA3.0-pri-miR-23a plasmid, ligated, and amplified in transformed bacteria.

For luciferase assays, HeLa cells were seeded in 24-well plates and co-transfected with 25 ng of luciferase reporter and/or 300 ng pcDNA3.0-based expression vector. After 48 h, cells were harvested for luciferase assays using the Luciferase Assay System (Promega, E1500). GLOMAX luminometer was used to collect light generated by Renilla or Firefly. For knockdown experiments, specific siRNA (20 nM) was transfected into HeLa cells 24 h ahead of the introduction of the luciferase reporter.

For producing recombinant His-tagged EWS in bacteria, EWS cDNA was subcloned into pET-32a between the EcoR I and Xho I sites. The plasmid was transformed into the *Escherichia coli* strain BL21 (DE3), which was induced with 0.5 mM isopropyl beta-D-1-thiogalactopyranoside (IPTG) for 3 h at 22°C. His-tagged EWS was purified on Ni-NTA beads, concentrated with Centricon (Millipore), and stored in 14 mM HEPES-pH 7.9, 90 mM KCl, 2.2 mM $MgCl_2$ and 30% glycerol until use.

CLIP-seq and RIP-PCR

EWS CLIP-seq was performed according to the published procedure (31,32). Briefly, HeLa cells cultured in a 150 mm plate were washed once with PBS followed by UV irradiation at 400 mJ/cm^2 under a HL-2000 Hybrilinker. Scrapped Cells were harvested by centrifugation at 500 g for 5 min at 4°C. Crosslinked cells were lysed in 500 μl of 1× PBS containing 0.1% SDS, 0.5% deoxycholate and 0.5% NP-40 on ice for 30 min. 30 μl of RQ1 DNAse I (Promega, M6101) was added to each tube, and incubated at 37°C for 2 min with rotation at 1000 rpm on a Theromixer. After chilling on ice for 5 min, supernatant was collected by centrifugation at 12 000 rpm for 20 min at 4°C. Immunoprecipitation was carried with 5 μg anti-EWS antibody. After Immunoprecipitation, Micrococcal Nuclease (MNase) of various dilutions was utilized to trim RNA and the reaction was terminated with EGTA. The 3′ linker labelled by gama-^{32}P-ATP was ligated to RNA-protein complexes before SDS-PAGE. After nitrocellulose transfer, the band above EWS was excised and treated with Proteinase K. The 5′ linker was then ligated to isolated RNAs. After PCR amplification for 18 cycles, the library was subjected to deep sequencing on Illumina HiSeq-2000.

Sequenced tags were mapped to the hg19 genome by Bowtie2 (33) and peak calling was performed as previously described (34). The complete set of RefGene from UCSC Table was used to calculate the tag distribution (35). Crosslinking-Induced Mutation Sites (CIMS) were identified as described (36). Local structure forming possibility was calculated by RNAplfold from ViennaRNA Package (37) around the peaks with height equal to or greater than 5, and then averaged by using the peak centre as pivot. PARIS data were from the published study (38). EWS–RNA interactions with peak height equal to or >5 were intersected with the PARIS data by BEDTools (39). Background sequences were generated by BEDTools shuffle (39).

For RNA immunoprecipitation (RIP), HeLa cells were treated with UV as in CLIP-seq. After immunoprecipitation and Proteinase K digestion, isolated total RNA was used for first-strand cDNA synthesis with SuperScript III reverse transcriptase (Life Technology) followed by N6 random priming. The resulting dsDNA was used for real-time PCR analysis using specific primers (listed in Supplementary Table S3).

MS2 capture

HeLa cells cultured in 100 mm plate were co-transfected with 10 μg plasmid expressing the eGFP-MS2 fusion protein and 15 μg individual MS2-pri-miRNA plasmids. After 48 h, cells were harvested and lysed in wash buffer (1× PBS-pH 7.4, 0.1% SDS, 0.5% deoxycholate, 0.5% NP40, 1 mM PMSF, 1 U/μl RiboLock RNase Inhibitor) on ice for 30 min. Cells were next treated with 30 μl of RQ1 DNase (Promega) at 37° for 2 min. The lysate was clarified by centrifugation at 12 000 rpm for 20 min at 4°C and collected supernatant was incubated with 5 μg anti-eGFP antibodies on Protein G Dynabeads (Life Technology) for 5 h at 4°C with rotation. The beads were washed three times with 1 ml wash buffer and three times with high-salt wash buffer (5× PBS-pH 7.4, 0.1% SDS, 0.5% deoxycholate, 0.5% NP40, 1 mM PMSF, 1 U/μl RiboLock RNase inhibitor). The captured product was fractionated by 10% SDS-PAGE followed by immunoblotting with the anti-EWS antibody.

In vitro transcription of RNA, gel shift, and *in vitro* pri-miRNA processing

We used pcDNA3.0-pri-microRNA plasmids to amplify templates for *in vitro* transcription of RNA with T7 RNA Polymerase (Fermentas) for gel shift assays. The primers are listed in Supplementary Table S4. *In vitro* transcribed RNAs (150 fmol) and purified EWS (0–0.24 pmol) were incubated at 30°C for 30 min in the reaction mix containing 0.5 μl RNase inhibitor, 1 μl 0.1% BSA and 1 μl reaction buffer (70 mM HEPES-pH 7.9, 450 mM KCl, 11 mM $MgCl_2$, 28% glycerol). At the end of the reaction, 1 μl 0.1% SYBR Green II was added and RNA–protein complexes were fractionated on 6% native polyacrylamide gel.

For *in vitro* pri-miRNA processing assays, purified RNA was incubated with immunoprecipitated Microprocessor from HEK293 cells expressing FLAG-DGCR8 according to the previously published protocol (40). Briefly, 15 μl immunoprecipitated Microprocessor was incubated in a 30 μl reaction mix containing 2 μl (0–4 μM) purified EWS, 100 ng RNA, 3 μl 64 mM $MgCl_2$, 1 μl 10 mM ATP, 1 μl RNase inhibitor at 37°C for 90 min. After proteinase K (Fermentas) treatment, RNA was extracted with phenol and precipitated with ethanol. Recovered RNA was fractionated on 8% denaturing gel and detected by northern blotting by using the DIG Northern Starter Kit (Roche, 12039672910) according to manufacturer's instruction. Briefly, after RNA fractionation and transfer onto nylon membrane, RNA was fixed with UV for 1 min, and after rising briefly with double distilled water, the membrane was baked at 80°C for 2 h. Pre-hybridization was performed with DIG Easy Hyb at 68°C for 4 h. DIG-labeled probes were generated by using specific primers (listed in Supplementary Table S4). After pre-hybridization, denatured DIG-labeled RNA probe was added and incubated at 68°C overnight. After washing twice, each for 5 min in 2× SSC, 0.1% SDS at 25°C, and then twice, each for 30 min in 0.1× SSC, 0.1% SDS at 68°C, the membrane was developed by the anti-DIG antibody. For northern blotting detection of mature miRNAs, DNA probes (listed in Supplementary Table S5) were labeled with DIG at 3′ end. After pre-hybridization, denatured probe was added and the reaction was incubated at 42°C overnight. After washing twice, each for 5 min in 2× SSC, 0.1% SDS at 25°C, and then twice, each for 30 min in 0.1× SSC, 0.1% SDS at 42°C, the membrane was developed by the anti-DIG antibody.

ChIP-qPCR

Cultured HeLa cells in a 100 mm plate were crosslinked with 1% formaldehyde at room temperature for 10 min and then stopped with 0.125 M glycine for 5 min. Scrapped cells were harvested by centrifugation at 500 g for 5 min at 4°C. Cells were resuspended in 0.3 ml of lysis buffer containing 1% SDS, 10 mM EDTA, 50 mM Tris–Cl, pH8.1, 1× protease inhibitor cocktail and sonicated three times for 10 s each at 150 W on ice. After decrosslinking at 65°C for 30 min,

2 μl of sonicated chromatin was taken to check the quality of chromatin, which should have most signals from 0.5 to 2 kb. Isolated chromatin was suspended in 1:10 (vol/vol) in dilution buffer (1% Triton X-100, 2 mM EDTA, 150 mM NaCl, 20 mM Tris–Cl, pH8.1, 1× protease inhibitor cocktail). Soluble chromatin was incubated at 4°C with 5 μg anti-Drosha (Abcam) overnight. DNA-protein complexes were captured on Protein G Dynabeads (Life Technology) for 3 h. Beads were sequentially washed for 10 min at 4°C with 1 ml of TSE I (20 mM Tris–HCl, pH 8.1, 0.1% SDS, 1% Triton X-100, 2 mM EDTA, 150 mM NaCl), 1 ml TSE II (20 mM Tris–HCl, pH 8.1, 0.1% SDS, 1% Triton X-100, 2 mM EDTA, 500 mM NaCl), and finally 1 ml TE buffer (10 mM Tris–Cl, pH 7.5, 1 mM EDTA). Complexes were eluted twice from the beads with 150 μl of 50 mM Tris-pH 8.0, 10 mM EDTA and 1% SDS. Decrosslinking was performed at 65°C overnight. DNA was purified with phenol and precipitated by ethanol in the presence of glycogen. Quantitative PCR was performed on CFX Connect PCR machine (BIO-RAD) using a SYBR green mix (TIANGEN) with specific primers (listed in Supplementary Table S3). The percentage of immunoprecipitated chromatin was calculated from ΔCt against input chromatin.

RESULTS

EWS binds a large subset of pri-miRNAs *in vivo*

To perform CLIP-seq for EWS in HeLa cells, we first confirmed the specificity of the anti-EWS antibody by western blotting before and after EWS knockdown with two independent siRNAs (Supplementary Figure S1A). Using this highly specific antibody, we carried out immunoprecipitation, showing quantitative recovery of endogenous EWS from HeLa whole cell extracts (Figure 1A, left panel). We next performed UV crosslinking on HeLa cells followed by ^{32}P-labeling of RNA crosslinked to EWS after immunoprecipitation. To obtain optimal RNA length for mapping and resolution, we treated the immunoprecipitate with increasing doses of MNase (Figure 1A, right panel) and identified a condition for isolating EWS-bound RNAs of ∼50 nt in length. The resulting RNA was subjected to linker ligation followed by PCR amplification according to the standard CLIP-seq protocol (31,41), yielding a total of 8.8 million tags, of which 3.8 million were uniquely mapped to the human genome. Analysis of Crosslinking Induced Mutation Sites (CIMS) showed the even distribution of deletions, but not insertions or substitutions, along the sequenced tags (Supplementary Figure S1B), characteristic of UV-induced mutation profiles (42), thus validating the general quality of our CLIP-seq data.

Consistent with early reports (10,18), most EWS–RNA interactions occurred in introns (57.9%) and intergenic regions (30.6%) (Figure 1B). Although we detected various GC-enriched sequence tags, we were unable to derive enriched consensus motifs, which have been similarly reported with individual TET family members (18). Instead, we noted many tags associated with pri-miRNAs, as illustrated (Figure 1C and Supplementary Figure S1C), suggesting that EWS may interact with some sort of secondary structures in RNAs, rather than specific motifs in single-stranded RNA regions. This prompted us to intersect the EWS CLIP-seq data with that generated by PARIS, a crosslinking-based strategy to map RNA duplexes in the genome (38). Indeed, EWS tags were co-incident with sequences with high base-pairing potentials (PARIS peaks), as illustrated (Figure 1D). About ∼40% of EWS peaks overlapped with PARIS-deduced RNA hairpins, which is significantly above the random background (Figure 1E). Aided with PARIS in searching for EWS-bound RNAs with secondary structures, we noted EWS binding clusters on ∼77 expressed pri-miRNAs. These data suggest that EWS binds a large subset of pri-miRNAs in HeLa cells.

Specific interaction of EWS with target pri-miRNAs

To verify the CLIP-seq results, we immunoprecipitated myc-tagged EWS from transfected HeLa cells and then selected a representative set of EWS target pri-miRNAs for RT-qPCR analysis in comparison with randomly picked non-target pri-miRNAs as control. We detected most EWS target pri-miRNAs we examined in the immunoprecipitate, although some were more abundant (i.e. miR-34a, miR-122 and miR-222) than others, likely reflecting their expression levels, but not GAPDH mRNA or various non-target pri-miRNAs we examined (Figure 2A). We made similar observation with RNA immunoprecipitation (RIP) assay using an antibody against endogenous EWS protein (Supplementary Figure S2A).

To demonstrate specific EWS recruitment to target pri-miRNAs, we performed a tethering assay by fusing three MS2 stem–loops with a pri-mRNA and co-expressing an eGFP-MS2 fusion protein in HeLa cells (illustrated in Figure 2B). This allowed us to use the anti-GFP antibody to pulldown the fusion protein and examine whether EWS could be captured via the MS2 stem–loop containing pri-miRNA. For this purpose, we selected two representative target pri-miRNAs (pri-miR-34a and pri-miR-222) and one negative control (pri-miR-23a). By pulling down eGFP with anti-GFP antibody, we indeed captured EWS on both pri-miR-34a and pri-miR-222, but not on control pri-miR-23a (Figure 2C). We verified this finding by three independent experiments (Supplementary Figure S2B). We conclude from this tethering experiment that EWS specifically binds a subset of pri-miRNAs in HeLa cells.

We next selected multiple pri-miRNAs to perform *in vitro* mobility shift assays with recombinant His-tagged EWS expressed and purified from bacteria. Consistent with the *in vivo* binding data, we detected specific interactions of EWS with all of the four target pri-miRNAs we examined, as indicated by the quantified results from three independent gel shift experiments (Figure 2D, top and middle panels, Supplementary Figure S2C). In contrast, we detected no shift with any of the five non-target pri-miRNAs we tested under the same conditions (Figure 2D, bottom panels, Supplementary Figure S2D). Together, these data demonstrate specific EWS binding to its target pri-miRNAs both *in vivo* and *in vitro*.

EWS is required for efficient expression of target miRNAs

To determine the functional impact of EWS binding on its target pri-miRNAs, we performed both EWS knock-

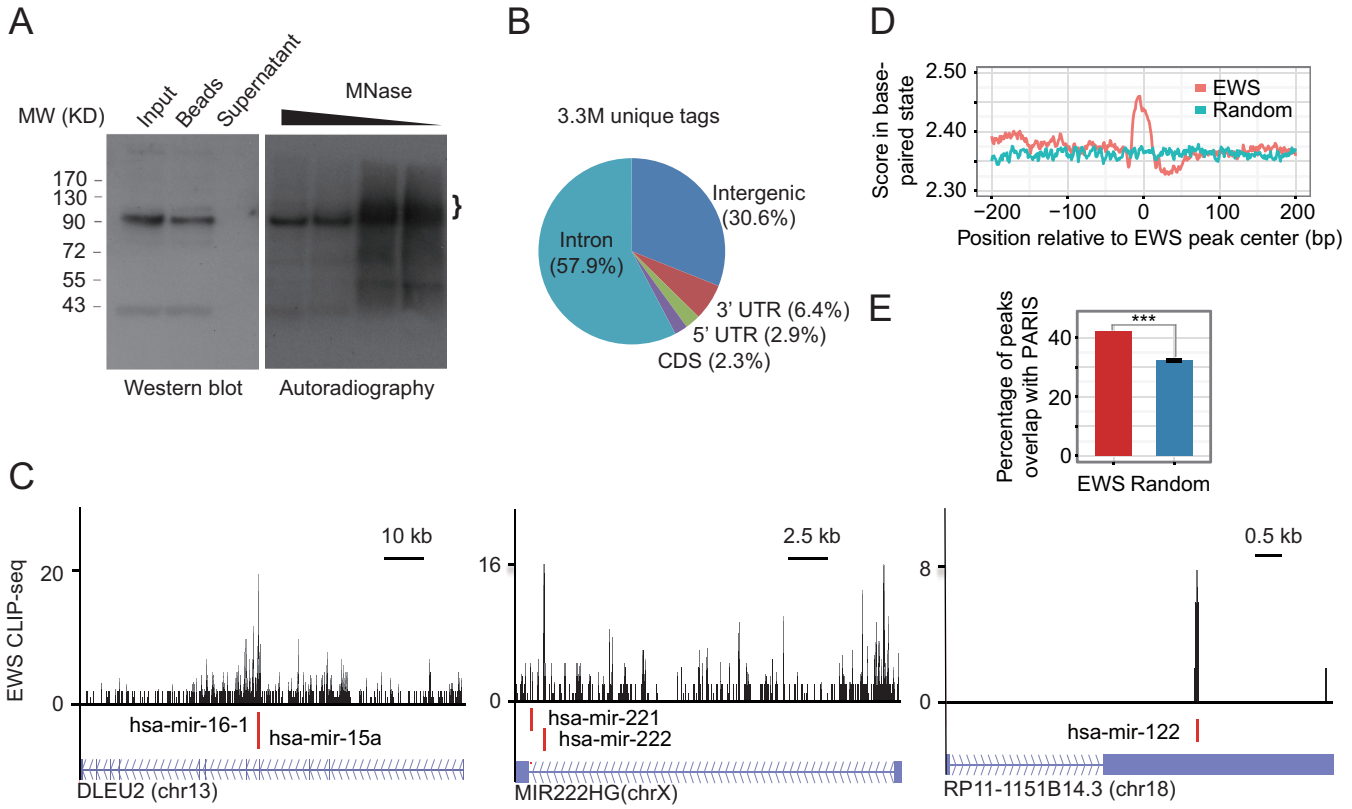

Figure 1. EWS binds a large subset of pri-miRNAs *in vivo*. (**A**) Western blot and phosphorimage of EWS–RNA complexes on SDS-PAGE. The immunoprecipitate was treated with decreasing concentrations of MNase to obtain optimal RNA-protein products that ensure both high mappability and resolution. The bracket indicates the excised complex for CLIP-seq library construction. (**B**) The genomic distribution of CLIP tags for EWS. (**C**) Representative EWS CLIP-seq binding events are shown on each gene model. (**D**) Local secondary structure forming possibility at positions relative to the center of EWS peaks. (**E**) Intersection of EWS binding events with the PARIS data compared to background to show the binding events correlated to the secondary structure. To determine the statistical significance, we computationally performed random sampling in the 'random' group for 100 times and then compared with one sample in the EWS group. Based on one sample Student's t test, we derived P-value $< 2.2e{-}16$ and presented the error bar as mean ± SD.

down and overexpression experiments. As previously reported (19), *EWS* knockdown elevated Drosha expression to a measurable degree, but had no effect on the expression of its cofactor DGCR8, as indicated by the quantified results based on three independent repeats of the experiment (Figure 3A, left panel; Supplementary Figure S3A). On the other hand, *EWS* overexpression did not seem to affect the level of either Drosha or DGCR8 (Figure 3A, right panel; Supplementary Figure S3B), implying that EWS knockdown-induced Drosha expression may result from an indirect mechanism. Under these conditions, we examined the expression levels of multiple EWS target and non-target pri-miRNAs by both semi-quantitative PCR and real time PCR and found none of them showed significant change in response to *EWS* knockdown or overexpression (Figure 3B and C). These results indicate that EWS is unlikely involved in transcriptional control of these pri-miRNAs.

We next performed real time PCR to examine the expression of mature miRNAs processed from these pri-miRNAs and found that seven out of nine miRNAs processed from EWS target pri-miRNAs were significantly reduced in response to *EWS* knockdown, with the remaining two miRNAs (miR-423 and miR-484) showing some trend of down-regulation but without sufficient statistical significance (Figure 3D). Conversely, all with one exception (miR-484) were significantly increased upon *EWS* overexpression (Figure 3E). None of miRNAs from non-target pri-miRNAs showed measurable changes under these conditions (Figure 3D and E). We further confirmed these trends by performing Northern blotting on four targets and two non-targets in response to *EWS* knockdown (Supplementary Figure S4) or overexpression (Supplementary Figure S5), all based on three independent experiments. Because *EWS* knockdown induced Drosha, we were intrigued by a possibility that some non-target miRNAs might be enhanced. We did not detect any enhancement among the set of non-target miRNAs we examined, implying that elevated Drosha might have selective effects on some, but not all expressed pri-miRNAs. Alternatively, Drosha level might not be a rate-limiting factor for pri-miRNA processing. Therefore, while future studies are required to understand how EWS might repress Drosha expression, our data strongly suggest that EWS has a positive role in miRNA biogenesis by selective binding to its target pri-miRNAs.

Conserved EWS function in miRNA biogenesis in HEK293 cells

To verify our observations on HeLa cells in terms of extensive interactions of EWS with pri-miRNA loci and its

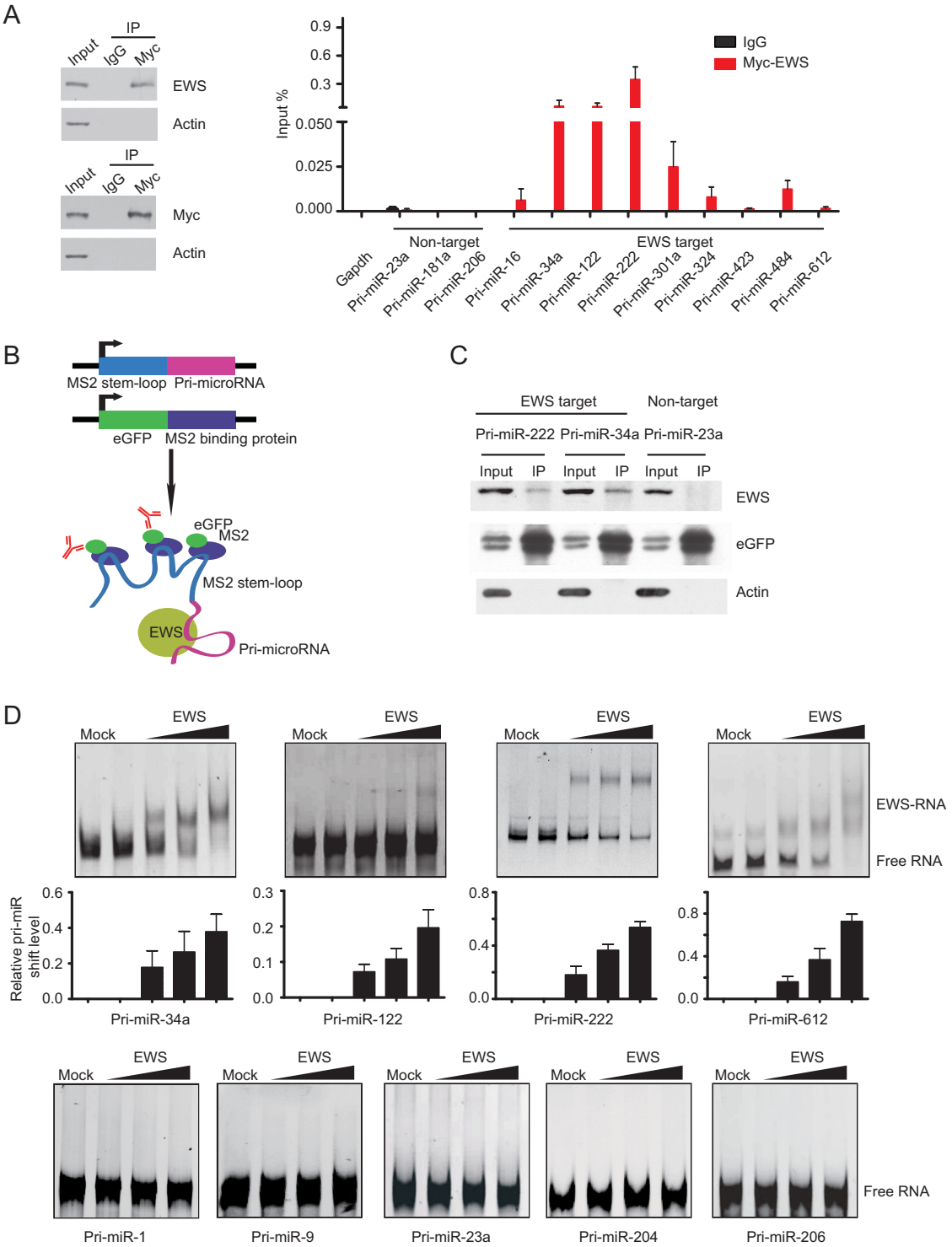

Figure 2. EWS interacts with specific target pri-miRNAs *in vitro*. (**A**) RIP analysis of EWS association of specific pri-miRNAs in HeLa cells. HeLa cells expressing myc-tagged EWS were immunoprecipitated with the anti-myc antibody (left). EWS-bound pri-miRNAs were detected by RT-qPCR (right). The percentage of immunoprecipitated pri-miRNA was calculated from ΔCt against input. Data are presented as mean ± SEM based on three independent experiments. (**B**) Diagram of the EWS pulldown strategy by MS2 tagged pri-miRNA. Each pri-miRNA was fused with three MS2 stem–loops, which was co-expressed with the eGFP-MS2 fusion protein in HeLa cells. By pulling down eGFP with anti-GFP antibody, we captured the MS2-pri-miRNA transcripts, which enabled us to examine the association of EWS with the pri-miRNAs. (**C**) Western blotting of the proteins from MS2-stem–loop/pri-miRNA pulldown by eGFP-MS2. EWS was detected on both pri-miR-34a and pri-miR-222, but not control pri-miR-23a. See two additional independent repeats of the experiments in Supplementary Figure S2B. (**D**) Gel shift analysis of EWS binding to multiple specific pri-miRNAs (upper panel), but not non-target pri-miRNAs (bottom panel). See two additional independent repeats of the experiments in Supplementary Figure S2C and S2D. Statistical significance of the quantified data was determined by two-tailed Student's t test based on three independent experiments and error bars were presented as mean ± SEM.

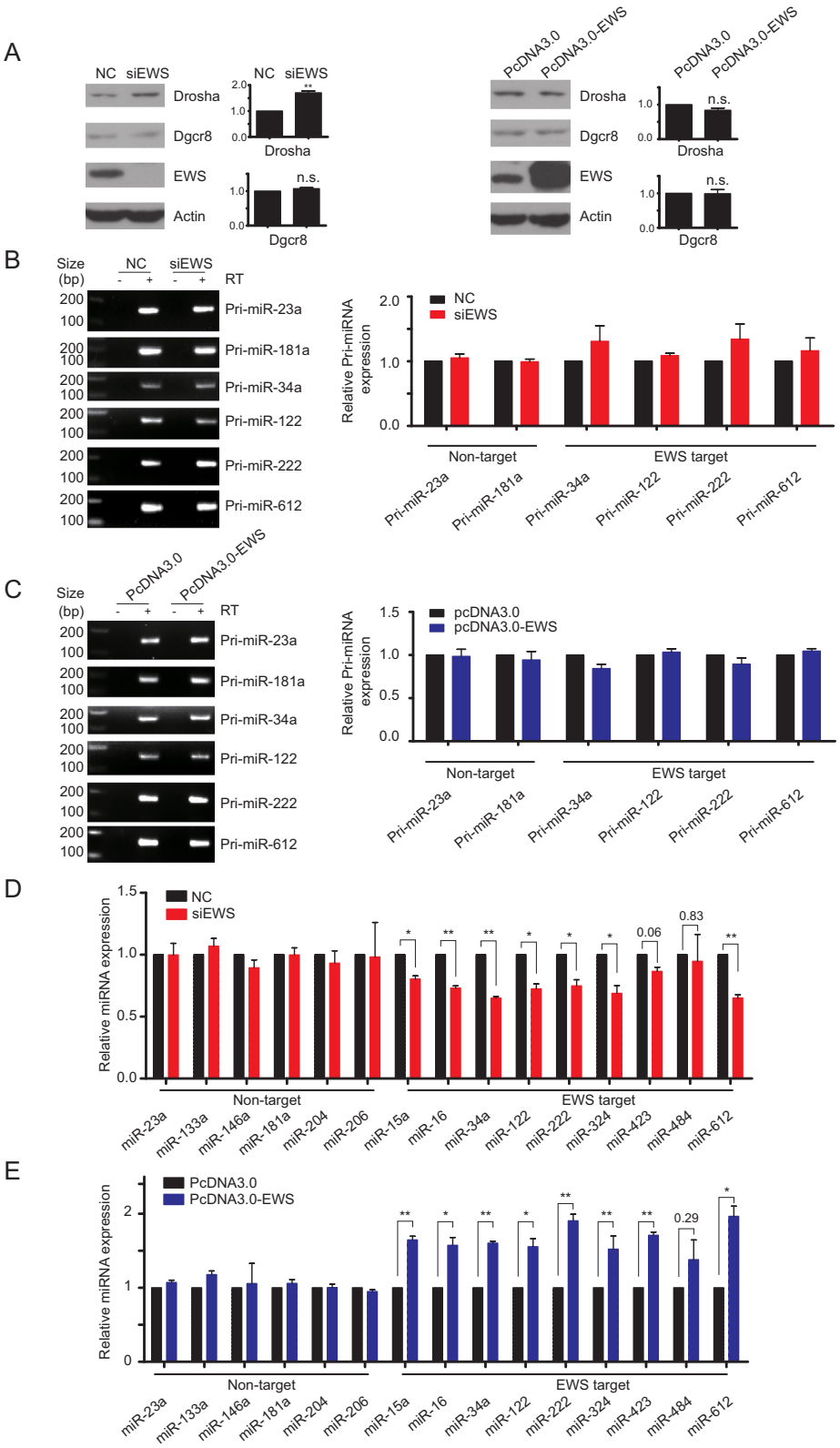

Figure 3. EWS is required for efficient expression of target miRNAs. (**A**) Western blotting analysis of EWS knockdown (left panels) or overexpression (right panels) and the levels of Drosha and DGCR8 under these experimental conditions. $^{**}P < 0.01$ based on three independent experiments; determined by two-tailed Student's *t* test, data are presented as mean ± SEM. (B, C) Expression levels of multiple target and non-target pri-miRNAs examined by semi-quantitative PCR (left panels) and real time PCR (right panels) with data presented as mean ± SEM in response to EWS knockdown (**B**) or overexpression (**C**). Relative pri-miRNA expression was normalized with GAPDH. (D, E) Significantly reduced and increased miRNAs from target pri-miRNAs, but not non-target pri-miRNAs, in response to EWS knockdown (**D**) or overexpression (**E**), respectively, in HeLa cells. Relative miRNA expression was normalized with U6. Statistical significance was determined by two-tailed Student's *t* test based on 3-independent experiments and error bars were presented as mean ± SEM. $^{*}P < 0.05$; $^{**}P < 0.01$. *P*-values that failed to meet the minimal level of 0.05 were specifically labelled on individual samples in panels D and E.

functional requirement for miRNA biogenesis, we took advantage of the existing EWS PAR-CLIP data on HEK293 cells (18). The Tuschl group expressed FLAG-HA-tagged *EWS* either constitutively (stable) or in an inducible fashion (inducible), generating 2.2M and 1.1M unique reads respectively under these conditions. Although these sequence depths on HEK293 cells were slightly lower than ours (3.8M) on HeLa cells, the use of a common anti-tag antibody for immunoprecipitation complemented our data generated using the antibody against the endogenous EWS protein. Analysis of both stable and inducible EWS data revealed 117 and 114 EWS binding peaks on pri-miRNAs with 74 in common between the two datasets. The seemly more prevalent EWS binding to pri-miRNAs in HEK293 cells is likely due to higher sensitivity of PAR-CLIP compared to standard CLIP-seq because of enhanced UV-crosslinking of 4-thiouridine containing RNAs with proteins (43). Despite cell type differences in pri-miRNA expression, we found that 36 pri-miRNAs were common targets for EWS between HeLa and HEK293 cells, demonstrating the prevalent interactions of EWS with a large number of pri-miRNAs in human cells.

We next selected a set of target and non-target pri-miRNAs (Figure 4A) to determine the production of mature miRNAs from these loci in response to *EWS* knockdown or overexpression. We found no effect on two clear non-targets (miR-133a and miR-204) and significant responses on 6 targets (miR-16, miR-34a, miR-122, miR-222, miR-423 and miR-484) in *EWS* knockdown cells, although two of these miRNAs (miR-16 and miR-122) did not reach to the standard statistical significance cut-off at P-value <0.05 (Figure 4B and C). Importantly, we observed two targets (miR-23a and miR-206) that did not robustly respond to *EWS* knockdown or overexpression in HEK293 cells. These observations, while largely consistent with our observations on HeLa cells, also imply that in certain cases, EWS binding does not necessarily lead to enhanced pri-miRNA processing.

Direct role of EWS in enhancing pri-miRNA processing

To determine a potential role of EWS in enhancing pri-miRNA processing, we designed a reporter-based assay by inserting individual pri-miRNA sequences in the 3′UTR of the Renilla luciferase reporter (Figure 5A). In this system, compromised pri-miRNA processing would increase Renilla expression relative to the Firefly reporter driven by a separate promoter, and enhanced pri-miRNA processing would produce the opposite effect, as described earlier (44–47). We verified this reporter system by knocking down *Drosha*, showing that all pri-miRNA reporters we tested elevated Renilla activities relative to Firefly activities (Supplementary Figure S6). We therefore utilized this reporter system to compare several EWS target pri-miRNAs with non-targets in HeLa cells. As expected, *EWS* knockdown enhanced the processing of the target pri-miRNAs, but not non-targets (Figure 5B), and conversely, *EWS* overexpression repressed the processing of the targets, but no non-targets (Figure 5C). These data strongly suggest a critical role of EWS in facilitating pri-miRNA processing.

To substantiate such direct role, we next performed *in vitro* pri-miRNA processing by using immunoprecipitated Microprocessor from HeLa cells expressing FLAG-tagged *DGCR8* (48,49), and tested recombinant His-tagged EWS for its activity in enhancing the reaction. By Northern blotting, we found that purified EWS was indeed able to enhance the processing of its target pri-miR-222 in a dosage-dependent manner (Figure 5D), but had no effect on a representative non-target pri-miR-23a (Figure 5E), which were further evidenced by the quantified data (bottom panels) from three independent pri-miRNA *in vitro* processing experiments (Supplementary Figure S7). Together with the results of the reporter-based assays in transfected cells, these data demonstrated a direct role of EWS in enhancing miRNA biogenesis at the pri-miRNA level.

Sequences flanking the stem–loop confer to the responsiveness to EWS

To understand how EWS might achieve its targeting specificity, we prepared various mutation or deletion constructs based on pri-miR-222 and tested *in vitro* transcribed RNAs for EWS binding by gel mobility shift. Comparing to native pri-miR-222 (Figure 6A, panel 1), we found that disruption of the stem–loop by replacing the 'star' strand of pri-miR-222 with the complementary strand dramatically reduced EWS binding (Figure 6A, panel 2). We similarly observed greatly compromised EWS binding with pri-miR-222 derived mutant RNAs in which either the loop region was deleted (Figure 6A, panel 3) or both flanking sequences removed (Figure 6A, panel 4). These data imply that multiple regions in pri-miR-222 contributed to EWS binding, reminiscent of some binding events that could not be linked to the functional requirement for EWS in HEK293 cells. It is also possible that drastically altered RNA secondary structure might underlie the reduced the affinity for EWS.

Because deletion of the flanking sequences was not expected to change RNA secondary structure, yet the mutation greatly diminished EWS binding, this suggests that compromised EWS binding may not necessarily be linked to altered RNA secondary structure. We next took advantage of pri-miR-23a, which seemed to be a non-target for EWS in HeLa cells (see Figure 2D and E), but clearly bound by EWS yet unable to respond to either EWS knockdown or overexpression in HEK293 cells (see Figure 4), to determine which sequence element(s) decisively contributes to the responsiveness to EWS. We therefore made two hybrid pri-miRNAs, one containing the stem/loop of pri-miR-222 but with the flanking sequences of pri-miR-23a (Figure 6B) and the other carrying the stem/loop of pri-miR-23a but with the flanking sequences of pri-miR-222 (Figure 6C). Gel shift with purified EWS showed that both hybrid RNAs bound EWS with comparable affinities (Figure 6B and C).

We next examined whether any of the hybrid pri-miRNAs responded to EWS-enhanced pri-miRNA processing *in vitro*. We found that the pri-miR-222 stem/loop linked with the pri-miR-23a flanking sequences was now processed in an EWS independent manner (Figure 6D), and in contrast, the fusion of the pri-miR-222 flanking sequences to the pri-miR-23a stem/loop rendered responsiveness to EWS (Figure 6E). These data were verified with three indepen-

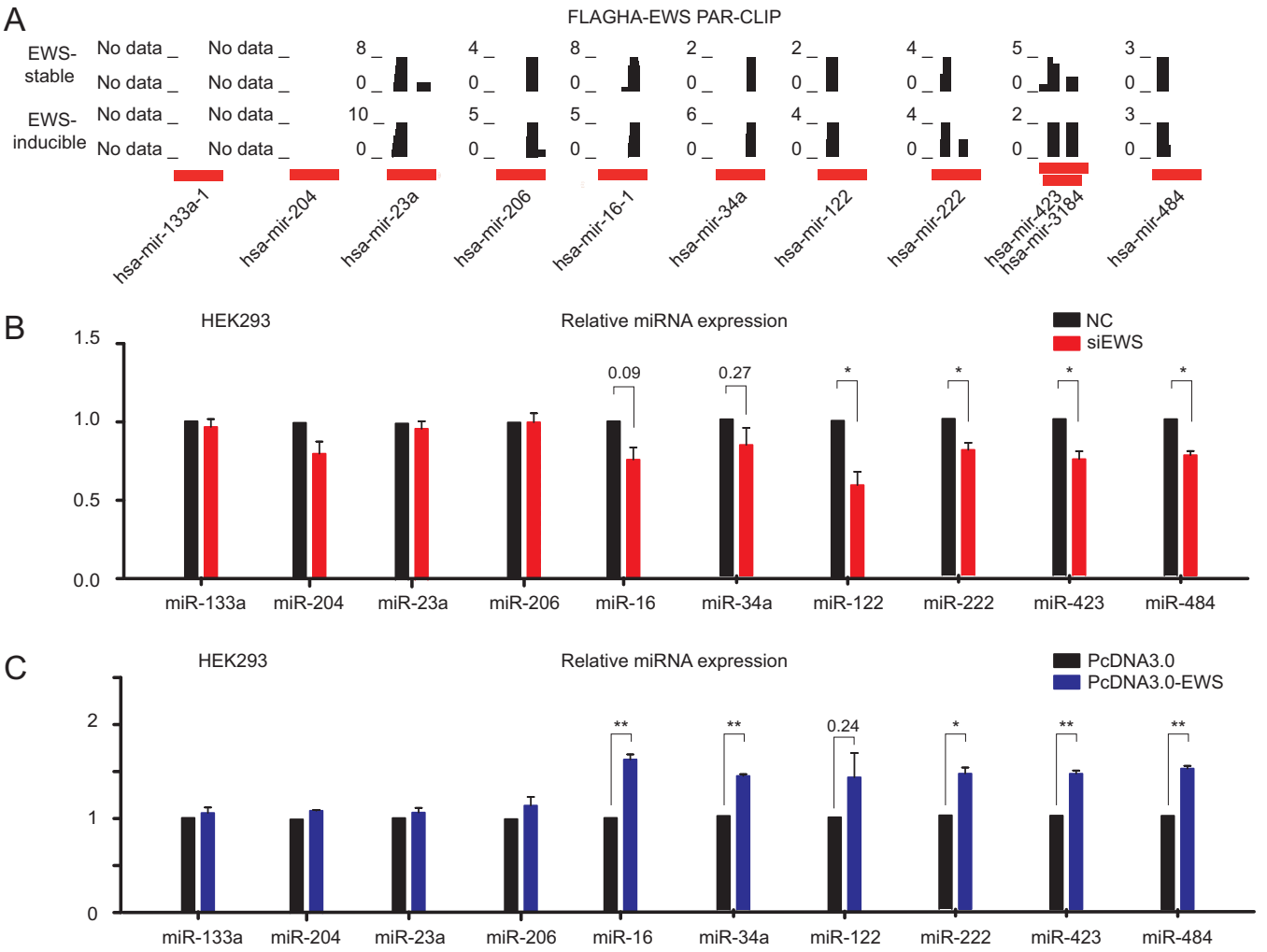

Figure 4. Conserved EWS function in miRNA biogenesis in HEK293 cells. (**A**) EWS binding on a set of pri-miRNAs based on the existing PAR-CLIP data generated from EWS-expressing HEK293 cells. EWS-stable: The data (SRR070460) from HEK293 cells constitutively expressing the FLAGHA-EWS; EWS-inducible: The data (SRR070461) from HEK293 cells after tetracyclin (Dox) induction of the tagged EWS. (B, C) Real-time PCR analysis of selective mature miRNAs in response to EWS knockdown (**B**) or overexpression (**C**), respectively, in HEK293 cells. Relative miRNA expression was normalized with U6. Statistical significance was determined by two-tailed Student's t test based on three independent experiments and error bars were presented as mean ± SEM. $*P < 0.05$; $**P < 0.01$. *P*-values that did not meet the minimal level of 0.05 were specifically labelled on individual samples in panels B and C.

dent *in vitro* pri-miRNA processing experiments (Supplementary Figure S8). We next tested both WT and chimeric pri-miRNA constructs in transfected HeLa cells to determine the importance of specific flanking sequences to confer EWS responsiveness *in vivo* (Figure 6F). We found that WT pri-miR-222 and the chimeric pri-miR-23a containing the flanking sequence of pri-miR-222 responded to *EWS* knockdown or overexpression whereas WT pri-miR-23a and the chimeric pri-miR-222 containing the flanking sequence of pri-miR-23a lacked the response. Together, these data demonstrate that EWS binding alone may not be sufficient to confer EWS-dependent pri-miRNA processing, and the flanking sequences in pri-miR-222 provides both binding specificity for and functional response to EWS in pri-miRNA processing by the Microprocessor.

EWS-dependent co-transcriptional recruitment of Drosha to target pri-miRNAs

Previous studies provided strong evidence for co-transcriptional pri-miRNA processing by the Microprocessor *in vivo* (20,21,50). It has also been shown that FUS/TLS facilitates co-transcriptional recruitment of Drosha to pri-miRNAs (50); however, it has been unclear whether such co-transcriptional recruitment of Drosha

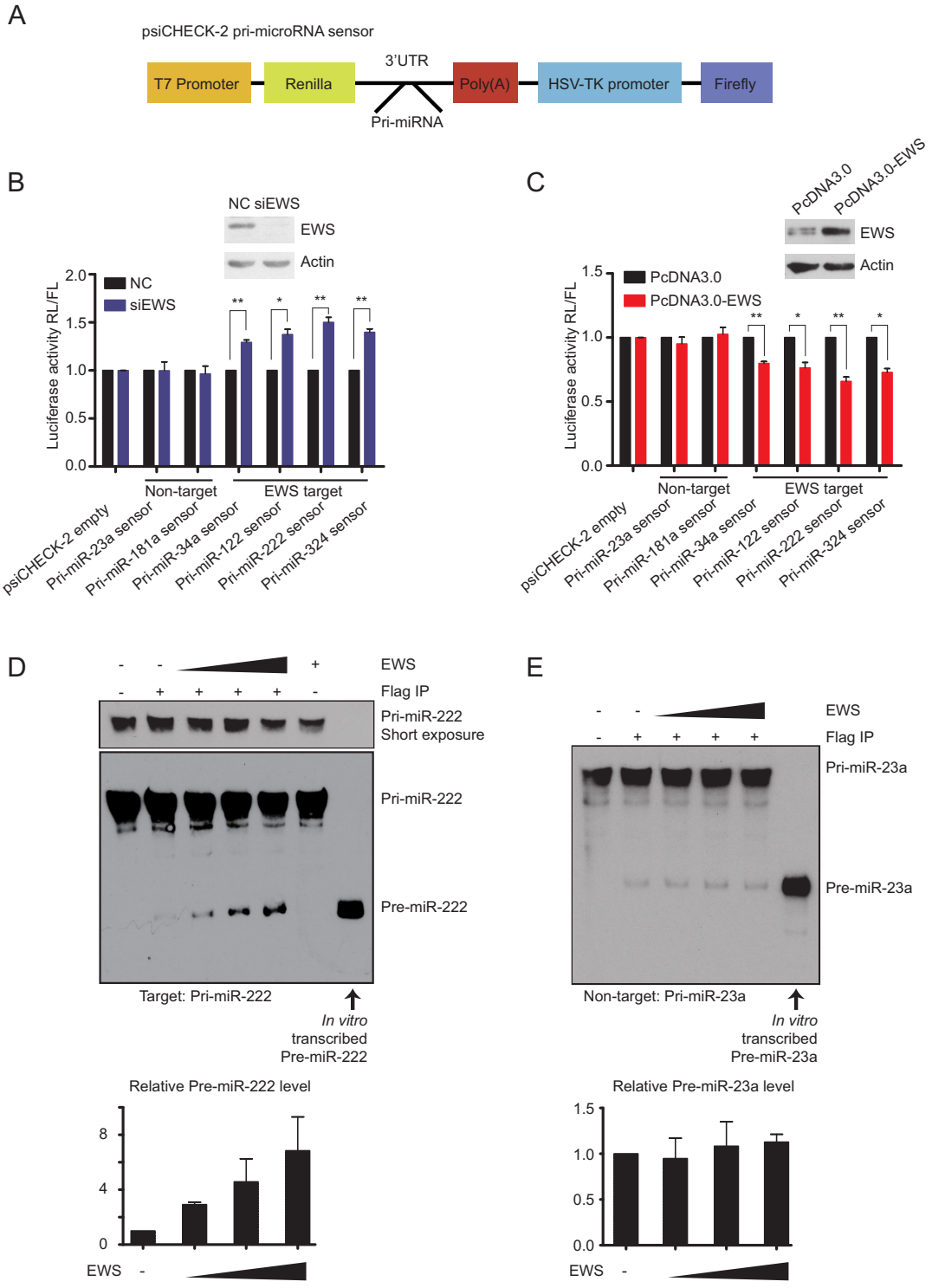

Figure 5. Direct role of EWS in enhancing target pri-miRNA processing. (**A**) Diagram of the reporter psiCHECK-2-based assay for pri-miRNA processing. Specific pri-miRNA sequences were inserted into the 3′UTR of Renilla luciferase reporter. Pri-miRNA processing will disrupt the 3′UTR of Renilla and thus decrease Renilla protein level. Compromised pri-miRNA processing would increase the Renilla luciferase activity relative to control Firefly luciferase. (B, C) Luciferase activities of HeLa cells transfected with individual pri-miRNA processing reporters in response to EWS knockdown (**B**) or overexpression (**C**). Statistical significance was determined by two-tailed Student's *t* test based on three independent experiments, data are presented as mean ± SEM. $*P < 0.05$; $**P < 0.01$. (D, E) Enhanced pri-miR-222 processing by immunoprecipitated Microprocessor from HeLa cells expressing FLAG-tagged DGCR8 in the presence of increasing amounts of recombinant EWS. *In vitro* transcribed pre-miR-222 as specific pre-miR marker was used for the processing assay and the products were detected by Northern blotting using a DIG-labelled pre-miR-222 probe (**D**). Parallel experiment was performed on a representative non-target pri-miR-23a (**E**). Relative processing bands were quantified. Statistical significance of the quantified data was determined by two-tailed Student's *t* test based on three independent experiments and error bars were presented as mean ± SEM. Two additional repeats of the experiments were shown in Supplementary Figure S7.

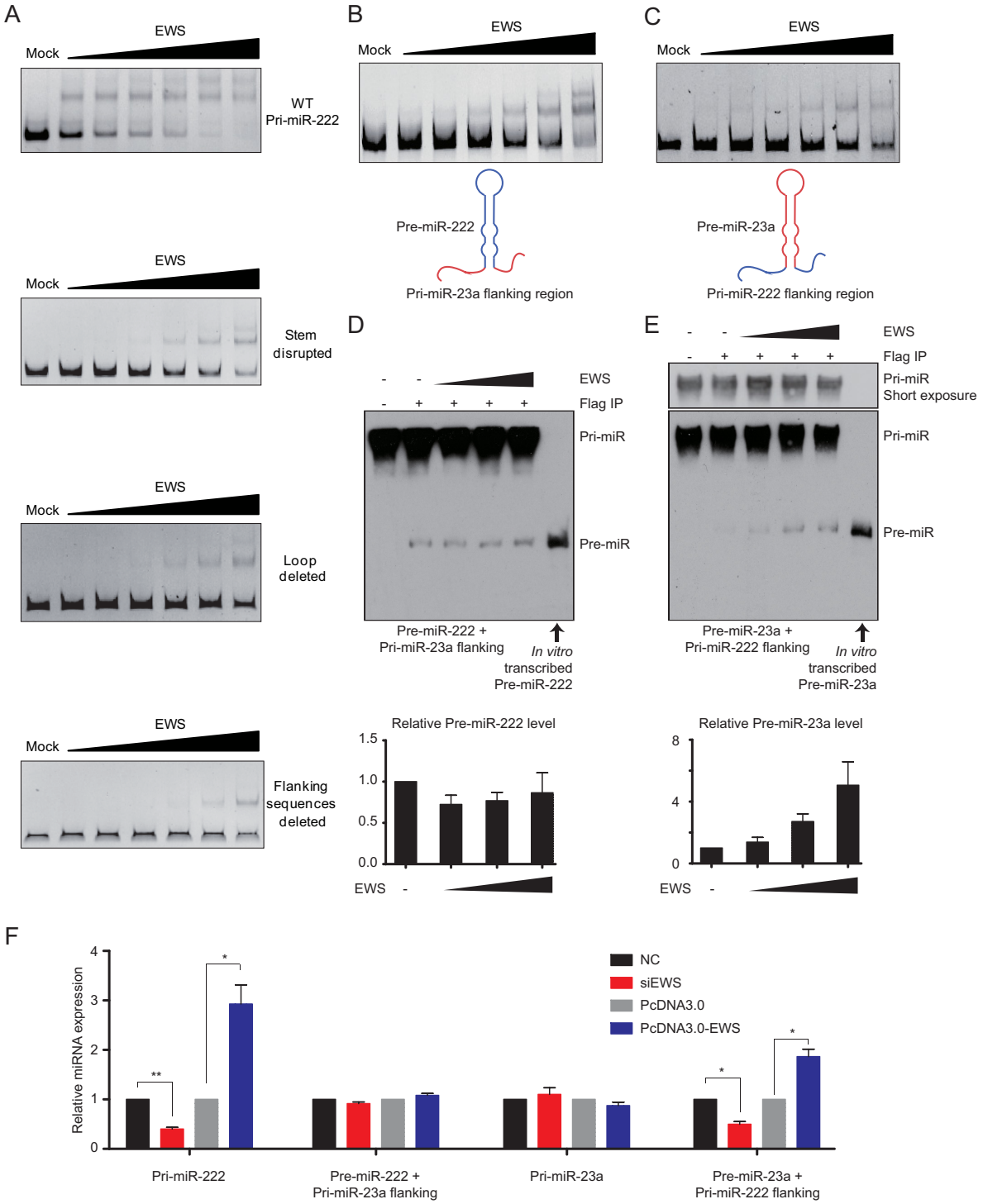

Figure 6. Sequences flanking the stem–loop provide EWS targeting specificity. (**A**) Gel shift analysis of EWS binding to wild-type and a series of mutant pri-miR-222. RNA-protein complexes were fractionated on 6% native polyacrylamide gel. Mutant pri-miR-222 analysed include disruption of its stem–loop, deletion of the loop region or removal of both flanking sequences. (B, C) Gel shift analysis of EWS binding to two reciprocal hybrid pri-miRNAs, one containing the stem/loop of pri-miR-222 in combination with the flanking sequences of pri-miR-23a (**B**) and the other carrying the stem/loop of pri-miR-23a in combination with the flanking sequences of pri-miR-222 (**C**). (D, E) *In vitro* processing of hybrid pri-miRNAs, pre-miR-222 carrying the flanking sequences of pri-miR-23a (**D**) or pre-miR-23a carrying the flanking sequences of pri-miR-222 (**E**) by immunoprecipitated Microprocessor in the presence of increasing amounts of EWS. *In vitro* transcribed pre-miR as specific marker was used for the processing assay. Relative processing bands were quantified. Two additional repeats of the experiments were shown in Supplementary Figure S8. (**F**) Real-time PCR analysis of mature miRNAs in response to EWS knockdown or overexpression in HeLa cells after transfection with WT or chimeric plasmids for 48 h. Relative miR-222 expression from WT (pri-miR-222) and its chimeric (pri-miR-23a+pre-miR-222 flanking) were normalized with U6. Relative miR-23a expression from WT (pri-miR-23a) and its chimeric (pri-miR-222+pre-miR-23a flanking) were normalized with U6. Statistical significance of the quantified data was determined by two-tailed Student's t test based on three independent experiments and error bars were presented as mean ± SEM. $*P < 0.05$; $**P < 0.01$.

depends on the ability of FUS/TLS to bind to DNA or RNA or both. To determine whether EWS functions in a similar fashion, we examined potential co-transcriptional recruitment of EWS to both its target and non-target pri-miRNAs by ChIP-qPCR. In this set of experiments, we first determined whether EWS could be detected on chromatin, finding that this was indeed the case, but EWS appeared to interact with chromatin underlying both target and non-target pri-miRNAs (Figure 7A).

We next investigated Drosha recruitment to the same chromatin regions in mock-treated or EWS-depleted HeLa cells. Because of slightly induced Drosha in EWS-depleted cells, we used relatively reduced cells from *EWS* knockdown cells to obtain roughly equal levels of Drosha in the immunoprecipitate, as indicated by western blotting (Figure 7B), and by ChIP-qPCR, we found that Drosha could be detected on chromatin of both EWS targets and non-targets (Figure 7C, black bars). Interestingly, such co-transcriptionally recruited Drosha appeared to be modestly enhanced on two out of four non-target pri-miRNAs (although the enhanced recruitment on pri-miR-181a did not meet the minimal *P*-value of 0.05) in response to *EWS* knockdown. This, coupled with de-repressed Drosha, might be responsible for induced miRNA expression in *EWS* knockdown mice (19), even though we have so far been unable to detect increased mature miRNAs from those non-target pri-miRNAs in HeLa cells (see Figure 3D). In any case, these data imply that EWS might indirectly suppress Drosha recruitment onto some non-target pri-miRNAs, although with an unknown mechanism at this point.

In control to non-target pri-miRNAs, Drosha recruitment to all EWS target pri-miRNAs we examined was reduced to various degrees in *EWS* knockdown cells, despite the fact that 3 out of 6 target pri-miRNAs did not reach the minimal *P*-value of 0.05 (Figure 7C). These data strongly suggest that EWS binding on its target pri-miRNAs stimulates co-transcriptional recruitment of Drosha to chromatin, thereby facilitating Drosha-mediated pri-miRNA processing, which may benefit from the direct interaction of EWS with its target pri-miRNAs.

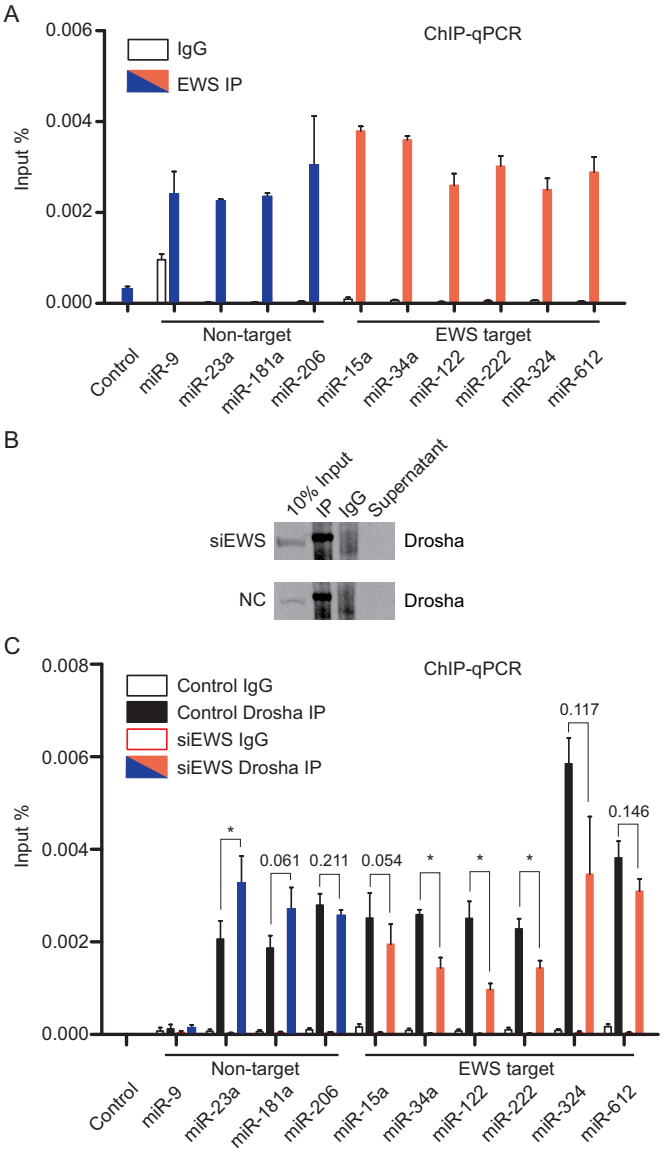

Figure 7. EWS binds to chromatin to enhance co-transcriptional recruitment of Drosha. (**A**) Anti-EWS ChIP-qPCR on chromatin regions of representative EWS target (orange) and non-target (blue) pri-miRNAs. HeLa cells were immunoprecipitated with anti-EWS antibodies. EWS-bound DNA was detected by qPCR. The percentage of immunoprecipitated pri-miRNA DNA was calculated from ΔCt against input. Data are presented as mean ± SEM based on three independent experiments. (**B**) Western blotting of Drosha, showing efficient immunoprecipitation of Drosha in both control and EWS knockdown cells. (**C**) Anti-Dosha ChIP-qPCR on chromatin regions of target (Orange) and non-target (Blue) pri-miRNAs before (black bars) and after (Orange/Blue bars) EWS knockdown. Statistical significance of the quantified data was determined by two-tailed Student's *t* test based on three independent experiments and error bars were presented as mean ± SEM. $*P < 0.05$. *P*-values that did not meet the minimal level of 0.05 were specifically labelled on individual experiments shown in panel C.

DISCUSSION

Enhancing Microprocessor activity and specificity by RBPs

Key machineries for miRNA biogenesis at individual steps have been well elucidated. The Microprocessor Drosha/DGCR8 is responsible for releasing individual pre-miRNAs from pri-miRNA transcripts; upon export to the cytoplasm, pre-miRNAs are further processed into mature miRNAs by Dicer/TRBP, which are finally incorporated into the RNA-induced silencing complex (RISC) for functional execution on target mRNAs (24). Importantly, each of these processing steps has been shown to subject to modulation by various RBPs (24) as well as by post-translational modification of the core machineries (51,52). Relevant to our current study, multiple RBPs have been implicated in the regulation of the Microprocessor-mediated conversion from pri-miRNA to pre-miRNA, including positive regulators, such as DDX5/17 (aka p68/p72) (53–56), hnRNP A1 (57,58), and KSRP (59), and negative regulators, such as Lin28 (60) and ADAR1/2 (61,62). We now provide evidence for a prevalent role of EWS in this process, acting to stimulate processing of a large number of pri-miRNAs by the Microprocessor.

EWS is a member of the TET family, and in fact, the other TET family member FUS/TLS has been shown to bind and stimulate processing of multiple pri-miRNAs (50). A role of EWS in enhancing pri-miRNA processing is consistent with the association of EWS with purified Microprocessor from a published mass spectrometric dataset (63). It is also interesting to note that FUS/TLS appears to bind the loop regions of its target pri-miRNAs, and by contrast, our current study shows that, while the loop region clearly contributes to high affinity binding of EWS to target pri-miRNA, it is their flanking sequences that confer the EWS responsiveness, likely due to EWS-assisted configuration of pri-miRNA for efficient Drosha cleavage. This is consistent with initial PAR-CLIP analysis of FUS/TLS (18) and our current CLIP-seq analysis of EWS, showing their preferential binding to RNAs with certain secondary structures. Because the TET family is also known to interact with one another in the cell (18,64–66), we may further speculate that multiple TET family members may function in a synergistic fashion on a subgroup of pri-miRNAs to enhance their biogenesis.

EWS regulation of miRNA biogenesis by two separate mechanisms

It is interesting to note that, while *EWS* knockdown induces Drosha expression (19), knockdown of *FUS/TLS* lacks such effect. Therefore, EWS likely modulates pri-miRNA processing in at least two levels. The induction of Drosha expression in *EWS* knockdown cells suggests a repressive role of this RBP at the level of transcription, which has been documented with the EWS-FLI1 fusion protein (67). This mechanism might account for the induction of a set of miRNAs in *EWS* knockout cells (19). However, since EWS overexpression failed to repress Drosha, it might be possible that EWS alone is insufficient to repress Drosha. In any case, we now show that EWS can also positively modulate miRNA biogenesis at the pri-miRNA level, thereby providing a potential mechanism for down-regulated miRNAs observed in *EWS* knockout cells.

Our data suggest that EWS is able to facilitate co-transcriptional recruitment of the Microprocessor to chromatin. Because pri-miRNA processing likely takes place co-transcriptionally (20,21), this may be a common theme for many RBPs involved in the regulation of miRNA biogenesis. Interestingly, we found that EWS is recruited to chromatin of both target and non-target pri-miRNAs, indicating that EWS-chromatin interactions likely reflect its role in transcription, which may take place ahead of co-transcriptional pri-miRNA processing. They may also account for EWS binding to some non-targets as we observed in HEK293 cells. Importantly, we found that chromatin-bound EWS is required for the enhanced recruitment of the Microprocessor to its target, but not non-target pri-miRNAs. Given the ability of EWS to directly interact with its target pri-miRNAs, we envision a potential synergy between co-transcriptional recruitment of the Microprocessor and loading of EWS from chromatin to newly transcribed pri-miRNAs to enhance their processing.

As discussed above, different TET family members appear to interact with one another via protein-protein interactions in the cell. This may enable some cross-regulation where more than one TET family members may similarly target some common chromatin regions, and such protein complex(s) may facilitate the recruitment of the Microprocessor to pri-miRNAs via different TET family members. This would create a network for different TET family members to regulate miRNA biogenesis in a combinatorial fashion in mammalian cells. Future studies will test this intriguing possibility.

EWS-regulated miRNA programs in development and disease

EWS has been demonstrated to play an important role in development and disease, such as cancer (15). As miRNAs are known to be widely involved in these biological processes and oncogenic transformation has been linked to repressed miRNA expression (68), such as LMTK3 (69), our findings provide a potential mechanism for the biological function of EWS via its role in the regulation of miRNA biogenesis. In Ewing Sarcoma, the *EWS* gene is frequently fused to the *FLI1* gene, an ETS family member, to acquire an oncogenic property (70–72). Although such fusion event has been widely assumed to affect the transcription activity of EWS, it will be interesting to investigate in future studies how such fusion protein may affect chromatin binding, thereby modulating the Microprocessor recruitment and/or co-transcriptional pri-miRNA processing, as part of the oncogenic property of the fusion protein.

A published study has also linked EWS to DNA damage induced by UV (9). The study provided evidence that UV irradiation induced EWS translocation to nucleolus, thus sequestrating EWS from the nucleoplasm, which might account for various induced alternative splicing events in UV-treated cells (9). In light of the role of EWS in pri-miRNA processing, it will be interesting to investigate in future studies how UV might also alter pri-miRNA processing via induced EWS redistribution in the cell or other mechanisms. Because EWS has been implicated in a wide range of biological processes, the newly elucidated function of EWS in miRNA biogenesis opens new doors to understanding potential disease mechanisms associated with this important RNA binding protein.

DATA AVAILABILITY

Sequenced CLIP-seq reads have been deposited in Gene Expression Omnibus under the accession numberr GSE90649.

SUPPLEMENTARY DATA

Supplementary Data are available at NAR Online.

ACKNOWLEDGEMENTS

We would like to thank Dr Jingyi Hui for sharing plasmid.

FUNDING

National Key R&D Program of China [2017YFA0504400]; Chinese 111 Program [B06018]; Chinese Academy of Science Foundation [22KJZD-EW-L12]; National Institutes of

Health [GM049369, HG004659, GM052872]. Funding for open access charge: National Key R&D Program of China [2017YFA0504400].
Conflict of interest statement. None declared.

REFERENCES

1. Law,W.J., Cann,K.L. and Hicks,G.G. (2006) TLS, EWS and TAF15: a model for transcriptional integration of gene expression. *Brief. Funct. Genomic Proteomic*, **5**, 8–14.
2. Tan,A.Y. and Manley,J.L. (2009) The TET family of proteins: functions and roles in disease. *J. Mol. Cell. Biol.*, **1**, 82–92.
3. Bertolotti,A., Lutz,Y., Heard,D.J., Chambon,P. and Tora,L. (1996) hTAF(II)68, a novel RNA/ssDNA-binding protein with homology to the pro-oncoproteins TLS/FUS and EWS is associated with both TFIID and RNA polymerase II. *EMBO J.*, **15**, 5022–5031.
4. Araya,N., Hirota,K., Shimamoto,Y., Miyagishi,M., Yoshida,E., Ishida,J., Kaneko,S., Kaneko,M., Nakajima,T. and Fukamizu,A. (2003) Cooperative interaction of EWS with CREB-binding protein selectively activates hepatocyte nuclear factor 4-mediated transcription. *J. Biol. Chem.*, **278**, 5427–5432.
5. Rossow,K.L. and Janknecht,R. (2001) The Ewing's sarcoma gene product functions as a transcriptional activator. *Cancer Res.*, **61**, 2690–2695.
6. Wang,X., Arai,S., Song,X., Reichart,D., Du,K., Pascual,G., Tempst,P., Rosenfeld,M.G., Glass,C.K. and Kurokawa,R. (2008) Induced ncRNAs allosterically modify RNA-binding proteins in cis to inhibit transcription. *Nature*, **454**, 126–130.
7. Yu,Y. and Reed,R. (2015) FUS functions in coupling transcription to splicing by mediating an interaction between RNAP II and U1 snRNP. *Proc. Natl. Acad. Sci. U.S.A.*, **112**, 8608–8613.
8. Lagier-Tourenne,C., Polymenidou,M., Hutt,K.R., Vu,A.Q., Baughn,M., Huelga,S.C., Clutario,K.M., Ling,S.C., Liang,T.Y., Mazur,C. *et al.* (2012) Divergent roles of ALS-linked proteins FUS/TLS and TDP-43 intersect in processing long pre-mRNAs. *Nat. Neurosci.*, **15**, 1488–1497.
9. Paronetto,M.P., Minana,B. and Valcarcel,J. (2011) The Ewing sarcoma protein regulates DNA damage-induced alternative splicing. *Mol. Cell*, **43**, 353–368.
10. Paronetto,M.P., Bernardis,I., Volpe,E., Bechara,E., Sebestyen,E., Eyras,E. and Valcarcel,J. (2014) Regulation of FAS exon definition and apoptosis by the Ewing sarcoma protein. *Cell Rep.*, **7**, 1211–1226.
11. Rogelj,B., Easton,L.E., Bogu,G.K., Stanton,L.W., Rot,G., Curk,T., Zupan,B., Sugimoto,Y., Modic,M., Haberman,N. *et al.* (2012) Widespread binding of FUS along nascent RNA regulates alternative splicing in the brain. *Sci. Rep.*, **2**, 603.
12. Kuroda,M., Sok,J., Webb,L., Baechtold,H., Urano,F., Yin,Y., Chung,P., de Rooij,D.G., Akhmedov,A., Ashley,T. *et al.* (2000) Male sterility and enhanced radiation sensitivity in TLS(-/-) mice. *EMBO J.*, **19**, 453–462.
13. Li,H., Watford,W., Li,C., Parmelee,A., Bryant,M.A., Deng,C., O'Shea,J. and Lee,S.B. (2007) Ewing sarcoma gene EWS is essential for meiosis and B lymphocyte development. *J. Clin. Invest.*, **117**, 1314–1323.
14. Ling,S.C., Polymenidou,M. and Cleveland,D.W. (2013) Converging mechanisms in ALS and FTD: disrupted RNA and protein homeostasis. *Neuron*, **79**, 416–438.
15. Paronetto,M.P. (2013) Ewing sarcoma protein: a key player in human cancer. *Int. J. Cell Biol.*, **2013**, 642853.
16. Kapeli,K., Pratt,G.A., Vu,A.Q., Hutt,K.R., Martinez,F.J., Sundararaman,B., Batra,R., Freese,P., Lambert,N.J., Huelga,S.C. *et al.* (2016) Distinct and shared functions of ALS-associated proteins TDP-43, FUS and TAF15 revealed by multisystem analyses. *Nat. Commun.*, **7**, 12143.
17. Modic,M., Ule,J. and Sibley,C.R. (2013) CLIPing the brain: studies of protein-RNA interactions important for neurodegenerative disorders. *Mol. Cell. Neurosci.*, **56**, 429–435.
18. Hoell,J.I., Larsson,E., Runge,S., Nusbaum,J.D., Duggimpudi,S., Farazi,T.A., Hafner,M., Borkhardt,A., Sander,C. and Tuschl,T. (2011) RNA targets of wild-type and mutant FET family proteins. *Nat. Struct. Mol. Biol.*, **18**, 1428–1431.
19. Kim,K.Y., Hwang,Y.J., Jung,M.K., Choe,J., Kim,Y., Kim,S., Lee,C.J., Ahn,H., Lee,J., Kowall,N.W. *et al.* (2014) A multifunctional protein EWS regulates the expression of Drosha and microRNAs. *Cell Death Differ.*, **21**, 136–145.
20. Morlando,M., Ballarino,M., Gromak,N., Pagano,F., Bozzoni,I. and Proudfoot,N.J. (2008) Primary microRNA transcripts are processed co-transcriptionally. *Nat. Struct. Mol. Biol.*, **15**, 902–909.
21. Ballarino,M., Pagano,F., Girardi,E., Morlando,M., Cacchiarelli,D., Marchioni,M., Proudfoot,N.J. and Bozzoni,I. (2009) Coupled RNA processing and transcription of intergenic primary microRNAs. *Mol. Cell. Biol.*, **29**, 5632–5638.
22. Winter,J., Jung,S., Keller,S., Gregory,R.I. and Diederichs,S. (2009) Many roads to maturity: microRNA biogenesis pathways and their regulation. *Nat. Cell. Biol.*, **11**, 228–234.
23. Krol,J., Loedige,I. and Filipowicz,W. (2010) The widespread regulation of microRNA biogenesis, function and decay. *Nat. Rev. Genet.*, **11**, 597–610.
24. Ha,M. and Kim,V.N. (2014) Regulation of microRNA biogenesis. *Nat. Rev. Mol. Cell. Biol.*, **15**, 509–524.
25. Ban,J., Jug,G., Mestdagh,P., Schwentner,R., Kauer,M., Aryee,D.N., Schaefer,K.L., Nakatani,F., Scotlandi,K., Reiter,M. *et al.* (2011) Hsa-mir-145 is the top EWS-FLI1-repressed microRNA involved in a positive feedback loop in Ewing's sarcoma. *Oncogene*, **30**, 2173–2180.
26. Tirode,F., Laud-Duval,K., Prieur,A., Delorme,B., Charbord,P. and Delattre,O. (2007) Mesenchymal stem cell features of Ewing tumors. *Cancer Cell*, **11**, 421–429.
27. Couthouis,J., Hart,M.P., Erion,R., King,O.D., Diaz,Z., Nakaya,T., Ibrahim,F., Kim,H.J., Mojsilovic-Petrovic,J., Panossian,S. *et al.* (2012) Evaluating the role of the FUS/TLS-related gene EWSR1 in amyotrophic lateral sclerosis. *Hum. Mol. Genet.*, **21**, 2899–2911.
28. Han,J., Pedersen,J.S., Kwon,S.C., Belair,C.D., Kim,Y.K., Yeom,K.H., Yang,W.Y., Haussler,D., Blelloch,R. and Kim,V.N. (2009) Posttranscriptional crossregulation between Drosha and DGCR8. *Cell*, **136**, 75–84.
29. Moffat,J., Grueneberg,D.A., Yang,X., Kim,S.Y., Kloepfer,A.M., Hinkle,G., Piqani,B., Eisenhaure,T.M., Luo,B., Grenier,J.K. *et al.* (2006) A lentiviral RNAi library for human and mouse genes applied to an arrayed viral high-content screen. *Cell*, **124**, 1283–1298.
30. Mo,S., Ji,X. and Fu,X.D. (2013) Unique role of SRSF2 in transcription activation and diverse functions of the SR and hnRNP proteins in gene expression regulation. *Transcription*, **4**, 251–259.
31. Xue,Y., Zhou,Y., Wu,T., Zhu,T., Ji,X., Kwon,Y.S., Zhang,C., Yeo,G., Black,D.L., Sun,H. *et al.* (2009) Genome-wide analysis of PTB-RNA interactions reveals a strategy used by the general splicing repressor to modulate exon inclusion or skipping. *Mol. Cell*, **36**, 996–1006.
32. Ule,J., Jensen,K., Mele,A. and Darnell,R.B. (2005) CLIP: a method for identifying protein-RNA interaction sites in living cells. *Methods*, **37**, 376–386.
33. Langmead,B. and Salzberg,S.L. (2012) Fast gapped-read alignment with Bowtie 2. *Nat. Methods*, **9**, 357–359.
34. Ji,X., Zhou,Y., Pandit,S., Huang,J., Li,H., Lin,C.Y., Xiao,R., Burge,C.B. and Fu,X.D. (2013) SR proteins collaborate with 7SK and promoter-associated nascent RNA to release paused polymerase. *Cell*, **153**, 855–868.
35. Kent,W.J., Sugnet,C.W., Furey,T.S., Roskin,K.M., Pringle,T.H., Zahler,A.M. and Haussler,D. (2002) The human genome browser at UCSC. *Genome Res.*, **12**, 996–1006.
36. Moore,M.J., Zhang,C., Gantman,E.C., Mele,A., Darnell,J.C. and Darnell,R.B. (2014) Mapping Argonaute and conventional RNA-binding protein interactions with RNA at single-nucleotide resolution using HITS-CLIP and CIMS analysis. *Nat. Protoc.*, **9**, 263–293.
37. Lorenz,R., Bernhart,S.H., Honer Zu Siederdissen,C., Tafer,H., Flamm,C., Stadler,P.F. and Hofacker,I.L. (2011) ViennaRNA Package 2.0. *Algorithms Mol. Biol.: AMB*, **6**, 26.
38. Lu,Z., Zhang,Q.C., Lee,B., Flynn,R.A., Smith,M.A., Robinson,J.T., Davidovich,C., Gooding,A.R., Goodrich,K.J., Mattick,J.S. *et al.* (2016) RNA duplex map in living cells reveals higher-order transcriptome structure. *Cell*, **165**, 1267–1279.
39. Quinlan,A.R. and Hall,I.M. (2010) BEDTools: a flexible suite of utilities for comparing genomic features. *Bioinformatics*, **26**, 841–842.
40. Lee,Y. and Kim,V.N. (2007) In vitro and in vivo assays for the activity of Drosha complex. *Methods Enzymol.*, **427**, 89–106.
41. Shao,C., Yang,B., Wu,T., Huang,J., Tang,P., Zhou,Y., Zhou,J., Qiu,J., Jiang,L., Li,H. *et al.* (2014) Mechanisms for U2AF to define 3′ splice

sites and regulate alternative splicing in the human genome. *Nat. Struct. Mol. Biol.*, **21**, 997–1005.
42. Zhang,C. and Darnell,R.B. (2011) Mapping in vivo protein-RNA interactions at single-nucleotide resolution from HITS-CLIP data. *Nat. Biotechnol.*, **29**, 607–614.
43. Hafner,M., Landthaler,M., Burger,L., Khorshid,M., Hausser,J., Berninger,P., Rothballer,A., Ascano,M. Jr, Jungkamp,A.C., Munschauer,M. *et al.* (2010) Transcriptome-wide identification of RNA-binding protein and microRNA target sites by PAR-CLIP. *Cell*, **141**, 129–141.
44. Wang,X., Zhao,X., Gao,P. and Wu,M. (2013) c-Myc modulates microRNA processing via the transcriptional regulation of Drosha. *Sci. Rep.*, **3**, 1942.
45. Weitz,S.H., Gong,M., Barr,I., Weiss,S. and Guo,F. (2014) Processing of microRNA primary transcripts requires heme in mammalian cells. *Proc. Natl. Acad. Sci. U.S.A.*, **111**, 1861–1866.
46. Allegra,D. and Mertens,D. (2011) In-vivo quantification of primary microRNA processing by Drosha with a luciferase based system. *Biochem. Biophys. Res. Commun.*, **406**, 501–505.
47. Allegra,D., Bilan,V., Garding,A., Dohner,H., Stilgenbauer,S., Kuchenbauer,F., Mertens,D. and Zucknick,M. (2014) Defective DROSHA processing contributes to downregulation of MiR-15/-16 in chronic lymphocytic leukemia. *Leukemia*, **28**, 98–107.
48. Lee,Y., Ahn,C., Han,J., Choi,H., Kim,J., Yim,J., Lee,J., Provost,P., Radmark,O., Kim,S. *et al.* (2003) The nuclear RNase III Drosha initiates microRNA processing. *Nature*, **425**, 415–419.
49. Han,J., Lee,Y., Yeom,K.H., Kim,Y.K., Jin,H. and Kim,V.N. (2004) The Drosha-DGCR8 complex in primary microRNA processing. *Genes Dev.*, **18**, 3016–3027.
50. Morlando,M., Dini Modigliani,S., Torrelli,G., Rosa,A., Di Carlo,V., Caffarelli,E. and Bozzoni,I. (2012) FUS stimulates microRNA biogenesis by facilitating co-transcriptional Drosha recruitment. *EMBO J.*, **31**, 4502–4510.
51. Warner,M.J., Bridge,K.S., Hewitson,J.P., Hodgkinson,M.R., Heyam,A., Massa,B.C., Haslam,J.C., Chatzifrangkeskou,M., Evans,G.J., Plevin,M.J. *et al.* (2016) S6K2-mediated regulation of TRBP as a determinant of miRNA expression in human primary lymphatic endothelial cells. *Nucleic Acids Res.*, **44**, 9942–9955.
52. Fletcher,C.E., Godfrey,J.D., Shibakawa,A., Bushell,M. and Bevan,C.L. (2016) A novel role for GSK3beta as a modulator of Drosha microprocessor activity and MicroRNA biogenesis. *Nucleic Acids Res.*, **45**, 2809–2828.
53. Moy,R.H., Cole,B.S., Yasunaga,A., Gold,B., Shankarling,G., Varble,A., Molleston,J.M., tenOever,B.R., Lynch,K.W. and Cherry,S. (2014) stem–loop recognition by DDX17 facilitates miRNA processing and antiviral defense. *Cell*, **158**, 764–777.
54. Salzman,D.W., Shubert-Coleman,J. and Furneaux,H. (2007) P68 RNA helicase unwinds the human let-7 microRNA precursor duplex and is required for let-7-directed silencing of gene expression. *J. Biol. Chem.*, **282**, 32773–32779.
55. Hong,S., Noh,H., Chen,H., Padia,R., Pan,Z.K., Su,S.B., Jing,Q., Ding,H.F. and Huang,S. (2013) Signaling by p38 MAPK stimulates nuclear localization of the microprocessor component p68 for processing of selected primary microRNAs. *Sci. Signal.*, **6**, ra16.
56. Wang,D., Huang,J. and Hu,Z. (2012) RNA helicase DDX5 regulates microRNA expression and contributes to cytoskeletal reorganization in basal breast cancer cells. *Mol. Cell. Proteomics*, **11**, M111 011932.
57. Guil,S. and Caceres,J.F. (2007) The multifunctional RNA-binding protein hnRNP A1 is required for processing of miR-18a. *Nat. Struct. Mol. Biol.*, **14**, 591–596.
58. Michlewski,G., Guil,S., Semple,C.A. and Caceres,J.F. (2008) Posttranscriptional regulation of miRNAs harboring conserved terminal loops. *Mol. Cell*, **32**, 383–393.
59. Trabucchi,M., Briata,P., Garcia-Mayoral,M., Haase,A.D., Filipowicz,W., Ramos,A., Gherzi,R. and Rosenfeld,M.G. (2009) The RNA-binding protein KSRP promotes the biogenesis of a subset of microRNAs. *Nature*, **459**, 1010–1014.
60. Hagan,J.P., Piskounova,E. and Gregory,R.I. (2009) Lin28 recruits the TUTase Zcchc11 to inhibit let-7 maturation in mouse embryonic stem cells. *Nat. Struct. Mol. Biol.*, **16**, 1021–1025.
61. Ota,H., Sakurai,M., Gupta,R., Valente,L., Wulff,B.E., Ariyoshi,K., Iizasa,H., Davuluri,R.V. and Nishikura,K. (2013) ADAR1 forms a complex with Dicer to promote microRNA processing and RNA-induced gene silencing. *Cell*, **153**, 575–589.
62. Chen,T., Xiang,J.F., Zhu,S., Chen,S., Yin,Q.F., Zhang,X.O., Zhang,J., Feng,H., Dong,R., Li,X.J. *et al.* (2015) ADAR1 is required for differentiation and neural induction by regulating microRNA processing in a catalytically independent manner. *Cell Res.*, **25**, 459–476.
63. Gregory,R.I., Yan,K.P., Amuthan,G., Chendrimada,T., Doratotaj,B., Cooch,N. and Shiekhattar,R. (2004) The Microprocessor complex mediates the genesis of microRNAs. *Nature*, **432**, 235–240.
64. Thomsen,C., Grundevik,P., Elias,P., Stahlberg,A. and Aman,P. (2013) A conserved N-terminal motif is required for complex formation between FUS, EWSR1, TAF15 and their oncogenic fusion proteins. *Faseb J.*, **27**, 4965–4974.
65. Zinszner,H., Albalat,R. and Ron,D. (1994) A novel effector domain from the RNA-binding protein TLS or EWS is required for oncogenic transformation by CHOP. *Genes Dev.*, **8**, 2513–2526.
66. Bertolotti,A., Melot,T., Acker,J., Vigneron,M., Delattre,O. and Tora,L. (1998) EWS, but not EWS-FLI-1, is associated with both TFIID and RNA polymerase II: interactions between two members of the TET family, EWS and hTAFII68, and subunits of TFIID and RNA polymerase II complexes. *Mol. Cell. Biol.*, **18**, 1489–1497.
67. De Vito,C., Riggi,N., Suva,M.L., Janiszewska,M., Horlbeck,J., Baumer,K., Provero,P. and Stamenkovic,I. (2011) Let-7a is a direct EWS-FLI-1 target implicated in Ewing's sarcoma development. *PLoS One*, **6**, e23592.
68. Lu,J., Getz,G., Miska,E.A., Alvarez-Saavedra,E., Lamb,J., Peck,D., Sweet-Cordero,A., Ebert,B.L., Mak,R.H., Ferrando,A.A. *et al.* (2005) MicroRNA expression profiles classify human cancers. *Nature*, **435**, 834–838.
69. Jacob,J., Favicchio,R., Karimian,N., Mehrabi,M., Harding,V., Castellano,L., Stebbing,J. and Giamas,G. (2016) LMTK3 escapes tumour suppressor miRNAs via sequestration of DDX5. *Cancer Lett.*, **372**, 137–146.
70. Bonin,G., Scamps,C., Turc-Carel,C. and Lipinski,M. (1993) Chimeric EWS-FLI1 transcript in a Ewing cell line with a complex t(11;22;14) translocation. *Cancer Res.*, **53**, 3655–3657.
71. Bailly,R.A., Bosselut,R., Zucman,J., Cormier,F., Delattre,O., Roussel,M., Thomas,G. and Ghysdael,J. (1994) DNA-binding and transcriptional activation properties of the EWS-FLI-1 fusion protein resulting from the t(11;22) translocation in Ewing sarcoma. *Mol. Cell Biol.*, **14**, 3230–3241.
72. May,W.A., Arvand,A., Thompson,A.D., Braun,B.S., Wright,M. and Denny,C.T. (1997) EWS/FLI1-induced manic fringe renders NIH 3T3 cells tumorigenic. *Nat. Genet.*, **17**, 495–497.